ELSEVIER

Biochimica et Biophysica Acta 1419 (1999) 33–42

BIOCHIMICA ET BIOPHYSICA ACTA
BBA

www.elsevier.com/locate/bba

Extracellular ATP-induced inward current in isolated epithelial cells of the endolymphatic sac

DaZheng Wu, Nozomu Mori *

Department of Otolaryngology, Kagawa Medical University, Kagawa 761-0793, Japan

Received 13 March 1998; received in revised form 17 March 1999; accepted 25 March 1999

Abstract

Using whole-cell patch-clamp technique and Fura-2 fluorescence measurement, the presence of ATP-activated ion channels and its dependence on intracellular Ca^{2+} concentration ($[Ca^{2+}]_i$) in the epithelial cells of the endolymphatic sac were investigated. In zero current-clamp configuration, the average resting membrane potential was -66.8 ± 1.3 mV ($n = 18$). Application of 30 μM ATP to the bath induced a rapid membrane depolarization by 43.1 ± 2.4 mV ($n = 18$). In voltage-clamp configuration, ATP-induced inward current at holding potential (V_H) of -60 mV was 169.7 ± 6.3 pA ($n = 18$). The amplitude of ATP-induced currents increased in sigmoidal fashion over the concentration range between 0.3 and 300 μM with a Hill coefficient (n) of 1.2 and a dissociation constant (K_d) of 11.7 μM. The potency order of purinergic analogues in ATP-induced current, which was 2MeSATP > ATPγs ≥ ATP > α,β-ATP > ADP = AMP ≥ adenosine = UTP, was consistent with the properties of the P_{2Y} receptor. The independence of the reversal potential of the ATP-induced current from Cl^- concentration suggests that the current is carried by a cation channel. The relative ionic permeability ratio of the channel modulated by ATP for cations was $Ca^{2+} > Na^+ > Li^+ > Ba^{2+} > Cs^+ = K^+$. ATP (10 μM) increased $[Ca^{2+}]_i$ in an external Ca^{2+}-free solution to a lesser degree than that in the external solution containing 1.13 mM $CaCl_2$. ATP-induced increase in $[Ca^{2+}]_i$ can be mimicked by application of ionomycin in a Ca^{2+}-free solution. These results indicate that ATP increases $[Ca^{2+}]_i$ through the P_{2Y} receptor with a subsequent activation of the non-selective cation channel, and that these effects of ATP are dependent on $[Ca^{2+}]_i$ and extracellular Ca^{2+}.

Keywords: Adenosine triphosphate; Endolymphatic sac; Non-selective cation conductance; Whole-cell patch-clamp; Fura 2

1. Introduction

The endolymphatic sac (ES) epithelium of the mammalian inner ear is presumed to absorb endolymphatic fluid generated from the stria vascularis in the cochlea and the dark cells in the vestibule organ, to regulate the endolymph volume, and to maintain the homeostasis of the endolymphatic system [1–3]. Recent investigations on ion transport in the ES epithelium have localized a (Na^++K^+)-ATPase at the basolateral membrane [4–6], a K^+ conductance at the basolateral and apical membranes [7] and an amiloride-sensitive Na^+ conductance at the apical membrane [8].

There is increasing evidence that ATP plays an important role as an extracellular messenger in many non-excitable and non-neuronal secretory cell types via different purinoceptors [9,10]. ATP stimulates secretion in both normal and cystic fibrosis airway epithelial cells [11] and in rat lacrimal cells [12].

* Corresponding author. Fax: +81 (87) 8912215;
E-mail: nozomu@kms.ac.jp

0005-2736/99/$ – see front matter
PII: S0005-2736(99)00053-X

It has been reported that ATP-activated channels were coupled with the ion transport mechanism in the epithelial cells of the kidney [13]. In the ES epithelial cells, however, the presence of ATP-activated channels has not been investigated.

Extracellular ATP exerts its effects through P2 receptors. Based on differences in molecular structure and signal transduction mechanisms, P2 receptors are divided into two families of ligand-gated ion channels and G protein-coupled receptors termed P2X and P2Y receptors, respectively [14]. To date seven mammalian P2X receptors ($P2X_{1-7}$) and five mammalian P2Y receptors ($P2Y_1$, $P2Y_2$, $P2Y_4$, $P2Y_6$, $P2Y_{11}$) have been cloned, characterized, and accepted as valid members of the P2 receptor family [14]. ATP-gated cation channels have been characterized on smooth muscle cells and autonomic and sensory neurons, where they mediate membrane depolarization and in some cases, Ca^{2+} entry [15–17]. Besides a direct activation of ion channels, ATP can induce a Ca^{2+} release from the inside of cells via IP_3-sensitive stores and then gate Ca^{2+}-activated ion channels including K^+, Cl^- and non-selective cation channels in the various cells [9].

In the present experiment we used the whole-cell patch-clamp method accompanied by Fura 2 fluorescence measurements to investigate the activation of cation channels by extracellular ATP in the ES epithelial cells. The results suggest that purinergic stimulation may activate non-selective cation channels by releasing Ca^{2+} from intracellular stores in the ES epithelial cells.

2. Methods and materials

2.1. Preparation

Healthy albino guinea pigs (300–400 g weight, Preyer reflex positive) of either sex were anesthetized with inhalation of diethyl ether and decapitated. The temporal bones were quickly removed and placed in oxygenated physiological saline solution after decapitation. Bony shell surrounding the endolymphatic duct and ES was peeled off carefully using a microelectric drill. Thereafter, the tissues were picked up with fine forceps under a stereomicroscope and kept in physiological saline solution containing (in mM) 140 NaCl, 5.4 KCl, 1.13 $CaCl_2$, 1.2 $MgCl_2$, 10 *N*-2-hydroxyethylpiperazine-*N*′-2-ethanesulfonic acid (HEPES), 10 D-glucose (pH 7.4), saturated with oxygen, for 30 min at room temperature (23 ± 2°C). Thereafter the intermediate portion of ES was separated by cutting the endolymphatic duct, and suspended in an isolation solution and incubated for 30 min at room temperature. The isolation solution was made by omitting calcium and adding 1 mM ethyleneglycol-bis(β-aminoethyl ether)-*N*,*N*,*N*′,*N*′-tetraacetic acid (EGTA), 0.2% bovine serum albumin and 100 units/ml collagenase (VIII) from a physiological saline solution. The ES was then transferred to the physiological saline solution containing 1.13 mM $CaCl_2$, in which the enzyme effect was stopped by washing the tissue for 30 min. The epithelial cells were isolated by gentle trituration with a siliconized Pasteur pipette. The epithelial cells were kept at room temperature and used within 3–5 h after the isolation.

This research was approved by the Animal Care and Use Committee of Kagawa Medical University under the heading 'Electrophysiological and Morphological Study of the Endolymphatic Sac in the Guinea Pig', and carried out in accordance with the Declaration of Helsinki.

2.2. Patch-clamp setup

Epithelial cells were allowed to settle on the glass floor of a chamber mounted on the stage of an inverted microscope (IMT-2, Olympus, Tokyo, Japan). The cells were classified into two types, large and small cells [18]. Whole-cell currents were recorded in the large cell by employing the standard patch-clamp techniques described by Hamill et al. [19]. The ES epithelial cells of the guinea pig are classified into two types according to ultrastructural findings [20]. The study using confocal laser microscopy [18] suggests that the large and small cells may correspond to type 1 and 2 cells [20], respectively. The micropipettes for patch-clamp recording were fabricated in two stages from blue-tip hematocrit glass on a vertical puller (Narishige, PP-83, Narishige Scientific, Tokyo, Japan) and fire-polished by a microforge (Narishige, MF-83, Narishige Scientific) to yield a tip diameter of approx. 1 μm. The pipette resistance ranged from 5 to 8 MΩ when filled with

145 mM KCl pipette solution in standard bath solution. The reference electrode in the bath was a silver-silver chloride coating wire, which was connected to the bath via a short bridge of the polyethylene tube filled with agar (20 mg/ml) dissolved in 3 M KCl solution. The pipette potential was balanced to the zero and junction potential was measured before seal formation on the epithelial cell. High-resistance seals were usually formed by placing the pipette tip in contact with the cell membrane and applying gentle suction. The seal was allowed to stabilize for 1–2 min, and the membrane patch was then ruptured using a slightly stronger suction to establish the conventional whole-cell configuration. The series resistance was compensated in all experiments. Membrane current (voltage-clamp configuration) and membrane potential (current-clamp configuration) were measured with a patch clamp amplifier (CEZ-2300, Nihon-Konden, Tokyo, Japan). Membrane currents were low-pass filtered at 0.5–2 kHz by the voltage-clamp amplifier. Data of membrane current and membrane potential were registered by a chart recorder (RECTI-HORIZ-8K, NEC San-Ei, Tokyo, Japan). All experiments were performed at room temperature.

2.3. Fluorescence measurement

Intracellular Ca^{2+} concentration ($[Ca^{2+}]_i$) in ES epithelial cells was measured using Fura 2 fluorescence according to the method described previously [21]. The cells were incubated in the extracellular solution with 5 μM Fura 2 acetoxymethyl ester (AM) for 60 min at room temperature. Fura 2-AM-loaded cells were then attached to the glass coverslip pretreated with Cell-Tak for 20 min. The coverslip was then attached to the base of a 120 μl perspex perfusion chamber mounted on the stage of an inverted microscope (TMD-EF, Nikon, Tokyo, Japan). Thereafter, the cells were continuously superfused at 37°C at a perfusion rate of 2 ml/min. Complete exchange occurred within several seconds. During the experiment the cells were illuminated alternately at excitation wavelengths of 340 and 380 nm, which were selected by the bandpass filters (band width = 10 nm) mounted on a rotating wheel. The excitation light source was provided by a 100 W mercury arc lamp. A neutral density filter was inserted in the excitation light path to decrease photobleaching. The excitation light was directed to the objective (Nikon 40X, oil immersion, numerical aperture: 1.30) by a dichroic mirror centered at 510 nm. The fluorescence emitted from the cells was collected by the above-mentioned objective, filtered by a 530 nM barrier filter, and monitored by a low-light, silicon-intensified target (SIT) camera (C-2400-7, Hamamatsu Photonics, Japan). The fluorescence images for each excitation wavelength were acquired at 10 s intervals. After subtraction of the background fluorescence, the ratio values of fluorescence image were analyzed by dividing the 340 nm image by the 380 nm image (F_{340}/F_{380}) with an image processor (Argus-50, Hamamatsu Photonics). An increased ratio of F_{340}/F_{380} indicates a rise of $[Ca^{2+}]_i$.

$[Ca^{2+}]_i$ was calculated from the fluorescence ratio in vivo by the following equation:

$$[Ca^{2+}]_i = K_d \times (R - R_{min})/(R_{max} - R)] \times \beta \quad (1)$$

where K_d is the dissociation constant of Fura 2 for calcium of 224 nM, R is the measured Fura 2 fluorescence ratio, R_{min} is the minimal fluorescence ratio determined by the addition of ionomycin (10 μM) to the cells in Ca^{2+}-free (5 mM EGTA) bath solution, and R_{max} is the maximal fluorescence ratio determined by the addition of ionomycin (10 μM) to the cells in a saturated Ca^{2+} control solution. β is the ratio of emission intensity with Ca^{2+}-free solution to that with a Ca^{2+}-saturated solution with excitation at 380 nm.

2.4. Solutions and chemicals

The standard pipette solution contained (in mM): KCl 140, $MgCl_2$ 1.2, HEPES 10, EGTA 0.5; pH was adjusted to 7.2 with KOH. The standard bath solution consisted of (in mM): 140 NaCl, 5.4 KCl, 1.2 $MgCl_2$, 1.13 $CaCl_2$, 10 HEPES, 5.0 D-glucose; pH was adjusted to 7.4 with NaOH. To measure the reversal potential (E_{rev}) of ATP-induced current, the pipette solution was made by replacing KCl with equimolar CsCl in the standard pipette solution. In the investigation of Na^+ dependence in ATP-induced current, low-Na^+ bath solutions were made by replacing NaCl and KCl with equimolar NMDG-Cl and CsCl in the standard bath solution, respectively. For measurement of the monovalent

cation permeability ratio, the external CsCl was replaced with 140 mM other cation species. For measurement of Ca^{2+} permeability, CsCl in the external solution was replaced with 23 mM $CaCl_2$ and 231 mM mannitol; the osmolarity was adjusted by addition of glucose. During the experiments a multibarreled polyethylene tube with a single outlet was placed within 200 μM of the cell. This tube allowed rapid solution changes for the introduction of chemicals. The perfusion rate of solutions was 2–3 ml/min. Complete exchange of the bath solution occurred within 10 s. Solutions were allowed to flow by gravity and were removed by aspiration from the recording chamber.

Fura 2-AM was purchased from Molecular Probes (Eugene, OR, USA). Cell-Tak was obtained from Collaborative Research (Bedford, MA, USA). 2-Methylthio-ATP (2MeSATP) was obtained from RBI Research Biochemicals (Natick, MA, USA). ATP (sodium salt), ADP (sodium salt), AMP (sodium salt), adenosine, α,β-methylene ATP (α,β-ATP) (lithium salt), uridine triphoshate (UTP) (sodium salt), adenosine 5′-*O*-(3-thiotriphosphate) (ATPγs), collagenase (type VIII), ionomycin, mannitol and bovine serum albumin were obtained from Sigma (St. Louis, MO, USA). Other agents were purchased from Wako Pure Chemicals (Tokyo, Japan).

2.5. Data analysis

Data are presented as means ± S.D. in the text and S.D. is indicated by a vertical bar in figures. Current-voltage (*I-V*) relationships were constructed from ATP-induced currents at a different holding potential. Ion permeability ratio of each cation to Cs^+ (P_X/P_{Cs}) for ATP-induced current was calculated from the constant field equations of Goldman-Hodgkin-Katz [22].

For monovalent cations:

$$P_X/P_{Cs} = ([Cs^+]_i/[X^+]_o) \times \exp(E_{rev}\, zF/RT) \quad (2)$$

For Ca^{2+} ions:

$$P_{Ca}/P_{Cs} = \{\exp(E_{rev}\, zF/RT) \times [\exp(E_{rev}\, zF/RT) + 1]\}/4 \quad (3)$$

where F, R, and T have their usual thermodynamic meanings, z is the ion valency, P_{Cs} is the Cs^+ permeability coefficient, $[X^+]_o$ was the test cation concentration in the bath solution, and $[Cs^+]_i$ corresponds to intracellular Cs^+ concentration. E_{rev} denotes the reversal potential obtained from *I-V* relationships of ATP-induced currents, which was determined by a second order polynomial expression fit to the data. R is equal to 8.314, F is equal to 9.648, and T is equal to 273.16 plus 23°C at room temperature. Con-

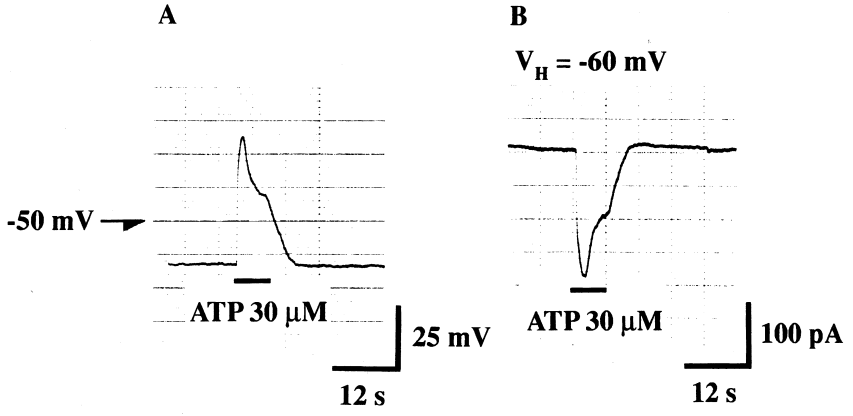

Fig. 1. ATP-induced membrane potential and current responses in the epithelial cells of the endolymphatic sac (ES). (A) Potential response induced by external application of ATP under current-clamp configuration. The resting potential was −67 mV. The epithelial cell was briefly exposed to 30 μM ATP for a period indicated by the horizontal bar below the response. The rapid membrane depolarization (from −67 to −19 mV) was induced by adding 30 μM ATP to the bath. Removal of ATP returned the membrane potential to the initial level. (B) ATP-induced inward current in ES epithelial cells under voltage-clamp configuration. The holding potential (V_H) was −60 mV. The horizontal bar below ATP exposure indicates the period for application of 30 μM ATP. A and B were recorded in the same cell.

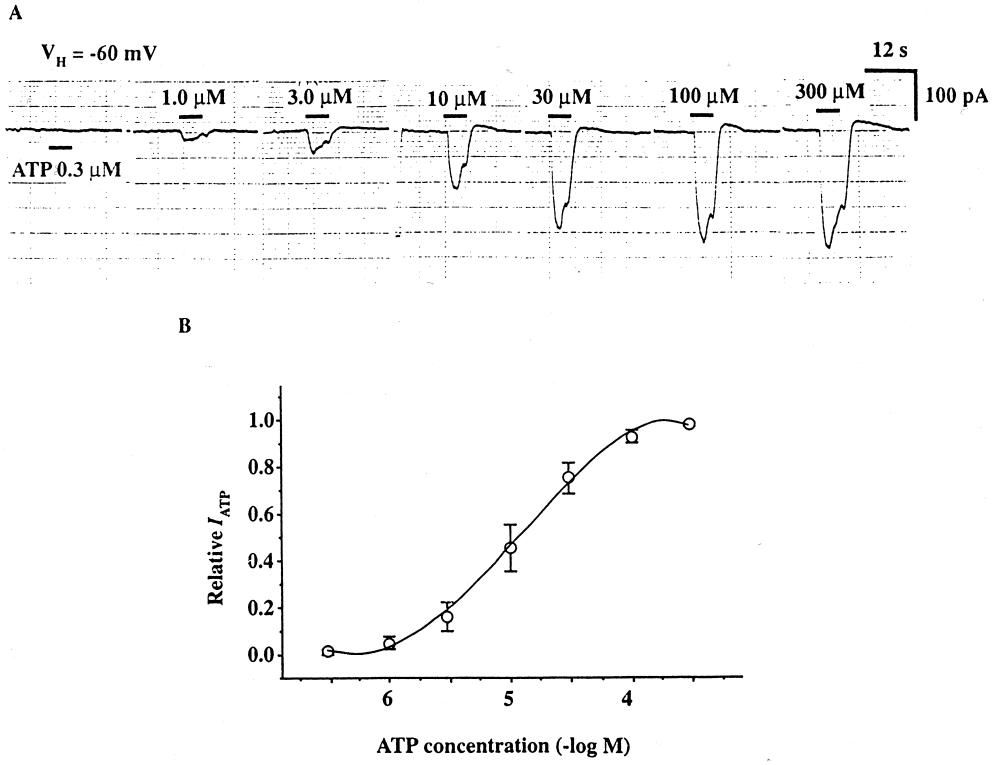

Fig. 2. Concentration-response relationship for ATP-induced inward current in ES epithelial cells. (A) Exogenous ATP at micromolar concentrations between 0.3 and 300 μM evoked a transient inward current, whose amplitude was increased in a dose-dependent manner. The horizontal black bars above and below the responses show the application period of ATP. Each response was recorded every 5 min in the same cell at a V_H of −60 mV. (B) Concentration-response curve for ATP-induced inward current. The continuous line was calculated from the Hill equation: $I/I_{max} = 1/[1+(K_d/C)^n]$, where K_d is the dissociation constant, C is ATP concentration, and n is the Hill coefficient (slope). K_d was 11.7 μM with n of 1.2. Vertical bars indicate mean ± S.D. ($n = 13$).

centration-response curves of ATP-induced currents were best fitted to data using the Hill equation:

$$I = I_{max}/[1 + (K_d/C)^n] \quad (4)$$

where I corresponds to ATP-induced currents, I_{max} to the maximum value of the current, n to the Hill coefficient, C to the ATP concentration and K_d to the apparent dissociation constant.

3. Results

3.1. ATP-induced inward currents

Isolated ES epithelial cells were perfused with 140 mM NaCl external solution, and the membrane potential was recorded with the standard pipette containing 145 mM KCl solution under current-clamp configuration. The value of the membrane potential in the isolated ES epithelial cells ranged from −57 to −67 mV with an average value of −66.8 ± 1.3 mV ($n = 18$). Application of 30 μM ATP to the bath induced a rapid membrane depolarization by 43.1 ± 2.4 mV (Fig. 1A). The membrane currents of the epithelial cells were measured at a holding potential (V_H) of −60 mV (near to the resting potential) under voltage-clamp configuration. The inward membrane current increased abruptly by adding 30 μM ATP to the bath (Fig. 1B). The value of ATP-induced currents in the isolated ES epithelial cells varied cell by cell and the average value was 169.7 ± 6.3 pA ($n = 18$). At V_H of −60 mV, ATP-induced current responses became detectable at a concentration of > 0.3 μM. Fig. 2A shows ATP-induced current responses at different concentrations of ATP. The concentration-response relationship of ATP-induced inward current showed

that the amplitude of ATP-induced currents increased in sigmoidal fashion over the concentration range between 0.3 and 300 μM (Fig. 2B). The solid line was fitted according to the Hill equation with a Hill coefficient (n) of 1.2 and a dissociation constant (K_d) of 11.7 μM.

3.2. Effects of ATP analogues

To determine the type of purinoceptors in ES epithelial cells, relative potencies of various purinergic analogues for ATP-induced currents were examined at V_H of −60 mV with the pipette containing

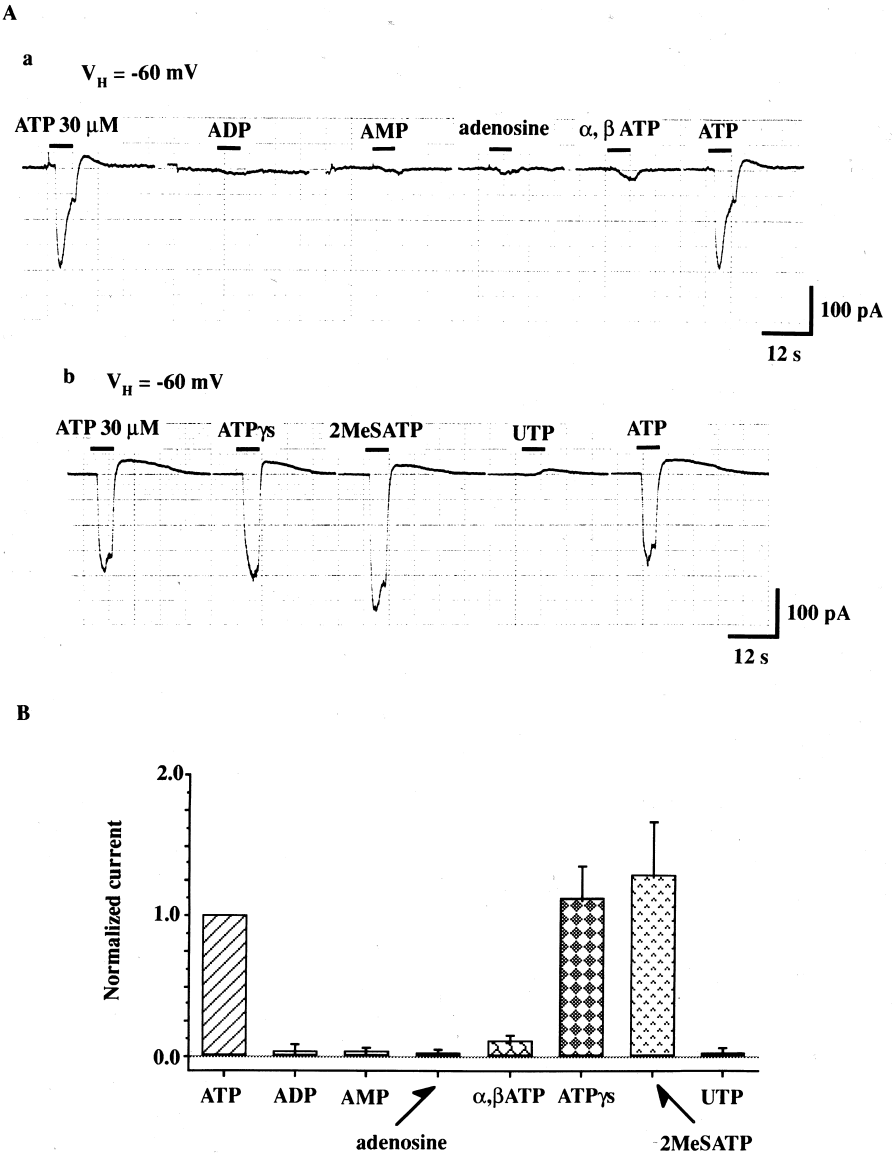

Fig. 3. ATP analogue-induced current. (A) Trace a: comparison of responses to ATP, ADP, AMP, adenosine, α,β-methylene-ATP (α,β-ATP) at 30 μM. The responses were obtained from the same cell at a V_H of −60 mV. Trace b: comparison of responses to ATP, adenosine-5′-*O*-(3-thiotriphoshate) (ATPγs), 2-methylthio-ATP (2MeSATP), and UTP at 30 μM. The responses were obtained from the same cell at a V_H of −60 mV. (B) Relative potency of purinergic agonists for the inward current induced at 30 μM concentration. Each value was normalized to the peak current induced by 30 μM ATP and expresses mean ± S.D. The agonist potency order was 2MeSATP > ATPγs ≥ ATP > α,β-ATP > ADP = AMP ≥ adenosine = UTP.

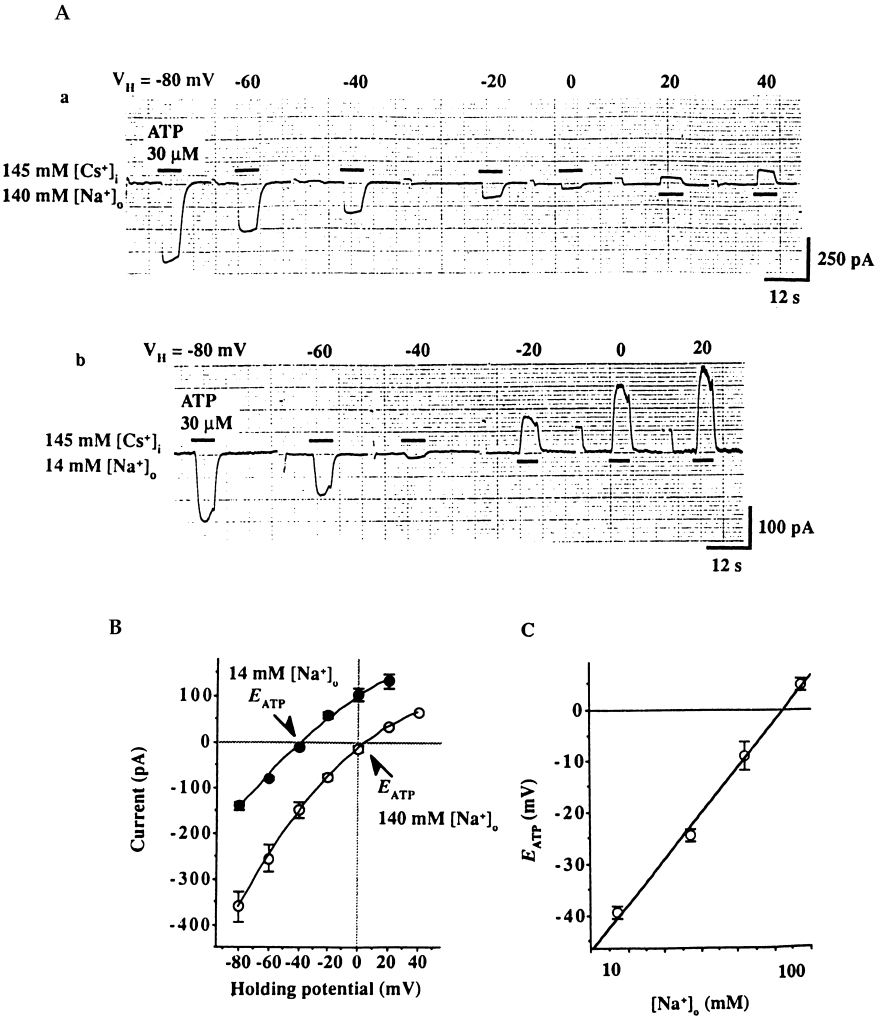

Fig. 4. Current-voltage (*I-V*) relationships for ATP-induced current. (A) Trace a: ATP-induced current at various V_H values in the same cell perfused with external and internal solutions containing 140 mM Na^+ and 145 mM Cs^+, respectively; trace b: ATP-induced current at various V_H values in the same cell perfused with external and internal solutions containing 14 mM Na^+ and 145 mM Cs^+, respectively. (B) *I-V* relationships for ATP-induced current in external solutions containing 14 mM (●) and 140 mM (○) Na^+ at a 145 mM Cs^+ pipette solution. (C) Relationship between E_{rev} (reversal potential of ATP-induced current; E_{ATP}) and $[Na^+]_o$. Means ± S.D. ($n=6$) of E_{rev} in different $[Na^+]_o$ are −50.3 ± 3.3 mV (1.4 mM), −39.6 ± 1.3 mV (14 mM), −24.5 ± 1.3 mV (35 mM), −9.0 ± 2.8 mV (70 mM), 4.7 ± 2.6 mV (140 mM). Data were fitted by least squares. Linear regression line (○) exhibits a slope of 45 mV/10-fold change in $[Na^+]_o$ from 140 to 14 mM.

145 mM KCl and the bath containing 140 mM NaCl. Each response was evoked at an interval of 5 min with 5 s application of 30 μM ATP or other purinergic agonists (Fig. 3A). ADP, AMP, adenosine and UTP only induced very small responses which were 4.5 ± 4.2% ($n=7$), 3.7 ± 2.3% ($n=7$), 2.6 ± 2.4% ($n=7$) and 3.0 ± 3.4% ($n=7$) of the control ATP-induced current, respectively. To further characterize the purine receptor subtypes, the responses to non-hydrolyzable ATP analogues were examined. α,β-ATP, a selective P_{2X} purinergic agonist, evoked a small response and its amplitude was 12 ± 3.0% ($n=8$) of the control ATP-induced current. 2MeSATP, a selective P_{2Y} purinergic agonist, could elicit a big response and its amplitude was 129.4 ± 37.3% ($n=8$) of the control ATP-induced current. ATPγs, a P_2 purinergic agonist, also could elicit a big response and its amplitude was 113.2 ± 22.6% ($n=8$) of the control ATP-induced current. The potency order of analogues was 2MeSATP > ATPγs ≥ ATP > α,β-

ATP > ADP = AMP ≥ adenosine = UTP, suggesting that ATP-induced inward current may be mediated by the P_{2Y} receptor in the ES epithelial cells.

3.3. Current-voltage relationships of ATP-induced responses

The average current-voltage (*I-V*) relationship of ATP-induced current was examined in various extracellular Na^+ concentrations ($[Na^+]_o$) at a constant 145 mM $[Cs^+]_i$. Cs^+ acts as a permeable ion. Fig. 4A shows typical current traces induced by 30 μM ATP at various V_H potentials in an external solution containing $[Na^+]_o$ of 140 mM and 14 mM. ATP-induced currents displayed a significant inward rectification and E_{rev} estimated from the intersection on the voltage axis of the *I-V* curve (E_{ATP}) was 4.7 ± 2.6 mV in 140 mM $[Na^+]_o$ and −39.6 ± 1.3 mV in 14 mM $[Na^+]_o$. Fig. 4C indicates the dependence of E_{rev} on $[Na^+]_o$. E_{rev} of ATP-induced current was determined at several $[Na^+]_o$. E_{rev} change in different $[Na^+]_o$ exhibited a slope of 45 mV/decade of Na^+ (open circles), which is rather less than the expected value of Na^+ selectivity (filled circles). Substitution of pipette Cl^- with aspartate$^-$ did not change E_{rev}, indicating that ATP-induced current is carried by a cation channel. If Na^+ is the main ion that could pass through the ATP-activated channel, the E_{rev} change should be 58 mV with a 10-fold change of $[Na^+]_o$ according to the Nernst equation: $E_{rev} = RT/F \times \ln([Na^+]_o/[Cs^+]_i)$. The E_{rev} change in the present experiment, however, is lower than the theoretical Nernst potential for Na^+, suggesting that the ATP-activated channel is permeable not only to Na^+ but also to other cations.

Table 1
Relative ion permeability ratio of ATP-induced current

$[X^+]_o$	*n*	E_{ATP} (mV)	P_X/P_{Cs}
Na^+	9	4.67 ± 2.64	1.25
K^+	8	−0.89 ± 1.14	1.00
Cs^+	6	0.04 ± 2.06	1.00
Li^+	4	2.53 ± 1.84	1.15
Rb^+	5	0.51 ± 1.75	1.07
Ca^{2+}	6	3.32 ± 2.01	3.24

Values are means ± S.E. for E_{ATP}. E_{ATP} is the reversal potential for ATP-induced current obtained from *I-V* plots as indicated in Section 2. $[X^+]_o$ is extracellular cation. Both pipette and bath solutions contained 145 mM Cs^+. For measurement of relative ion permeability ratio (P_X/P_{Cs}), 145 mM Cs^+ in the external solution was replaced by equimolar Na^+, K^+, Li^+, or Rb^+. For measurement of P_{Ca}/P_{Cs}, Ca^{2+} in the external solution was raised to 21.13 mM.

3.4. Ion permeability ratio

ATP-induced current was determined in a pipette filled with 145 mM CsCl. To measure the monovalent cation permeability ratio, the external CsCl was replaced with 140 mM other cation species. To measure P_{Ca}/P_{Cs}, CsCl in the external solution was replaced with 23 mM $CaCl_2$ and 231 mM mannitol; the osmolarity was adjusted by addition of glucose. E_{rev} was evaluated from *I-V* curves obtained for ATP-induced current. Ion permeabilities relative to Cs^+ were calculated from the value of E_{rev} using the Goldman-Hodgkin-Katz equation, assuming that the currents were carried by cations (see Table 1). The sequence of ion permeabilities obtained for ATP-induced current was $Ca^{2+} > Na^+ > Li^+ > Ba^+ > Cs^+ = K^+$.

3.5. $[Ca^{2+}]_i$ increased by ATP

The ATP-induced increase in $[Ca^{2+}]_i$ in the epithelial cells was measured by the amplitude of the fluorescence ratio (F_{340}/F_{380}) in the cells loaded with Fura 2-AM. In the standard external solution containing 1.13 mM $CaCl_2$ ATP increased $[Ca^{2+}]_i$ transiently from 81 ± 42 to 361 ± 104 μM ($n = 14$). Multiple application of ATP eliminated the $[Ca^{2+}]_i$ response. In Ca^{2+}-free external solution ATP increased $[Ca^{2+}]_i$ from 81 ± 42 to 202 ± 106 μM ($n = 14$), which was less than that in the external solution containing 1.13 mM $CaCl_2$ (Fig. 5A). The result indicates that the $[Ca^{2+}]_i$ increase by ATP is dependent on the extracellular Ca^{2+}. The decline of $[Ca^{2+}]_i$ response by multiple application of ATP suggests that intracellular Ca^{2+} stores can be rapidly depleted after the removal of extracellular Ca^{2+}. To test this possibility, the $[Ca^{2+}]_i$ response was examined by application of ionomycin in the absence of $[Ca^{2+}]_o$. After the first induction of the $[Ca^{2+}]_i$ response by application of ATP, 1.0 μM ionomycin changed $[Ca^{2+}]_i$ from 116 ± 63 to 400 ± 141 μM ($n = 7$) after approx. 1 min incubation with Ca^{2+}-free solution (Fig. 5B). The result indicates that a rise in $[Ca^{2+}]_i$ is due to Ca^{2+} release from internal pools.

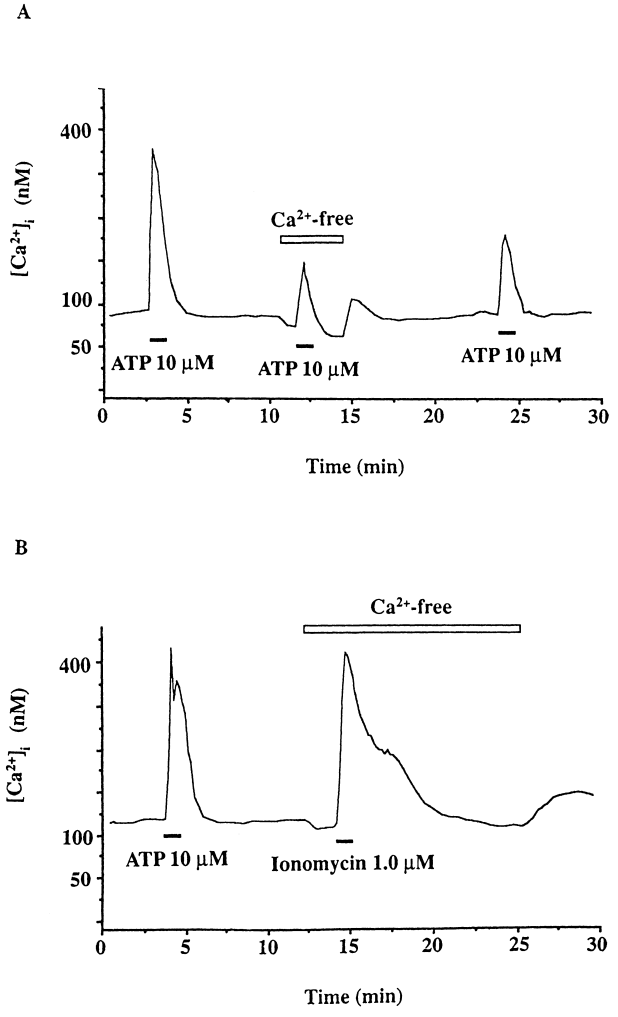

Fig. 5. (A) ATP-induced $[Ca^{2+}]_i$ increase in the presence and absence of extracellular Ca^{2+} ($[Ca^{2+}]_o$). The response to 10 μM ATP was reduced approx. 30 s after preincubation with Ca^{2+}-free solution containing 0.1 mM EGTA and showed a partial recovery after the switch to the standard bath solution containing 1.13 mM Ca^{2+}. (B) Effect of 1.0 μM ionomycin on $[Ca^{2+}]_i$ response in the absence of $[Ca^{2+}]_o$. Ionomycin induced a transient rise in $[Ca^{2+}]_i$ approx. 1 min after incubation with Ca^{2+}-free solution containing 0.1 mM EGTA. The ionomycin-induced $[Ca^{2+}]_i$ response gradually returned to the initial value during Ca^{2+}-free solution.

4. Discussion

The present study showed that in the ES epithelial cells of the guinea pig the extracellular ATP activates a cation channel via P2 receptor. The membrane depolarization under current-clamp configuration and whole-cell currents under voltage-clamp configuration induced by ATP are associated with the inward conductance increase. The *I-V* relationship of ATP-induced current exhibited an inward rectification with an E_{rev} of 5 mV. E_{rev} near 5 mV suggests that ATP may activate a cation channel. This possibility is supported by the fact that E_{rev} for ATP-induced current was dependent on $[Na^+]_o$. When replacing extracellular Na^+ with $NMDG^+$ (an impermeable cation), E_{rev} of the ATP-induced current shifted to a negative direction with a change in 45 mV per 10-fold decrease in $[Na^+]_o$. This property is consistent with a channel equally permeable to Na^+ and K^+. The sequence order of relative ion permeability for this cation channel calculated by the constant field equation was $Ca^{2+} > Na^+ > Li^+ > Ba^+ > Cs^+ = K^+$, indicating that the ATP-activated ion channel in the ES epithelia is permeable to monovalent and divalent cations. The relative ion permeability ratio of P_{Na}/P_{Cs} and P_{Ca}/P_{Cs} was 1.25 and 3.24, respectively. The results indicate that the ATP-activated channel is more permeable to Ca^{2+} than to Na^+. ATP-activated channels could be permeable to Ca^{2+} to a greater degree, assuming that cation channels could accelerate the increase in intracellular Ca^{2+}.

P2 receptors have been subdivided into five distinct subtypes (P_{2X}, P_{2Y}, P_{2U}, P_{2T} and P_{2Z}) according to their pharmacological profiles [9,14]. The potency order of purine receptor agonists for ATP-induced inward currents was 2MeSATP > ATPγs ≥ ATP > α,β-ATP > ADP = AMP ≥ adenosine = UTP. The results suggest that ATP-induced inward current in the ES epithelial cells may occur via P_{2Y} receptor. Purine receptors have been reported to be coupled to G protein, which leads to the production of inositol 1,4,5-trisphosphate (IP_3) [10]. ATP-induced channel is mediated by G proteins and phospholipase C in rat hepatocytes [23]. After ATP binds to a P_{2Y} receptor, Ca^{2+} release from intracellular pools might be induced through the activation of G protein with a subsequent production of IP_3. ATP can directly open a non-selective channel by increasing intracellular free Ca^{2+} in the membrane in a number of other tissues [24–26]. It has also been proposed that this channel can also allow the influx of Ca^{2+}, which can then activate other Ca^{2+}-dependent processes, such as increases in Cl^- or K^+ conductance [25–27].

The ATP-induced increase in $[Ca^{2+}]_i$ in ES epithelial cells loaded with Fura 2 was dependent on the

presence of extracellular Ca^{2+}. Elimination of extracellular Ca^{2+} significantly decreased the enhancement of intracellular Ca^{2+} induced by ATP. The ATP-induced increase in intracellular Ca^{2+} can be mimicked by application of ionomycin. These results indicate that the ATP-induced increase in intracellular Ca^{2+} might originate both from intracellular pools and from influx of extracellular Ca^{2+}, and that the release of Ca^{2+} from internal stores may be in conjunction with the activation of a Ca^{2+} influx pathway, a supplement of Ca^{2+} released from internal stores. Then the increased level of Ca^{2+} may activate a non-selective channel. The increase in the membrane permeability to Ca^{2+} and intracellular Ca^{2+} including trigger cellular signal transduction would induce Na^{+} influx and K^{+} efflux when the extracellular ATP was released to reach the ES epithelial cells. Thus, ATP-induced cation conductance may play an important role in maintaining homeostasis and regulating the ion transport process in ES epithelial cells.

There are increasing lines of evidence that ATP may play several roles in the modulation of the endolymphatic system [28–32]. The presence of ATP in the cochlear fluids [28] and a substantial localization of purinoceptors in the tissues lining the endolymphatic compartment [29] have been reported. Extracellular ATP is more sensitive to the cochlear endolymphatic compartment than to the perilymphatic compartment [30]. P_{2U} receptor has been reported to be localized in the apical membrane of the vestibular dark cells of the gerbil [31]. Although the present study did not demonstrate the localization of receptors, apical purinoceptors may explain more easily the involvement of ATP in maintaining homeostasis and regulating the ion transport process in ES epithelial cells.

Acknowledgements

This work was supported by Grants-in-Aid (Nos. 05454462 and 08671969) for Scientific Research from the Ministry of Education, Science and Culture of Japan.

References

[1] R.S. Kimura, H.F. Schuknecht, Pract. Otorhinolaryngol. 27 (1965) 343–354.
[2] P.G. Lundquist, Acta Otolaryngol. (Stockh.) 201, (Suppl.) (1965) 1–108.
[3] D. Bagger-Sjöbäck, H. Rask-Andersen, Am. J. Otol. 7 (1986) 134–140.
[4] F. Mizukoshi, D. Bagger-Sjöbäck, H. Rask-Andersen, J. Wersäll, Acta Otolaryngol. (Stockh.) 105 (1988) 202–208.
[5] H. Yamane, Y. Nakai, Adv. Otorhinolaryngol. 42 (1988) 123–128.
[6] W.J.F. ten Cate, L.M. Curtis, K.E. Rarey, ORL 56 (1994) 257–262.
[7] D. Wu, N. Mori, Am. J. Physiol. 271 (1996) C1765–C1773.
[8] N. Mori, D. Wu, Pflügers Arch. 443 (1996) 58–64.
[9] G.R. Dubyak, C. El-Moatassim, Am. J. Physiol. 265 (1993) C577–C606.
[10] S.E. O'Connor, I.A. Dainty, P. Leff, Trends Pharmacol. Sci. 12 (1991) 137–141.
[11] M.J. Stutts, T.C. Chinet, S.J. Mason, J.M. Fullton, L.L. Clarke, R.C. Boucher, Proc. Natl. Acad. Sci. USA 89 (1992) 1621–1625.
[12] P. Vincent, J. Physiol. 449 (1992) 313–331.
[13] B. Nilius, J. Sehrer, S. Heinke, G. Droogmans, Am. J. Physiol. 269 (1995) C376–C384.
[14] V. Ralevic, G. Burnstock, Pharmacol. Rev. 50 (1998) 413–492.
[15] B.P. Bean, C.A. Williams, P.W. Ceelen, J. Neurosci. 10 (1990) 11–19.
[16] C.D. Benham, R.W. Tsien, Nature 328 (1987) 275–278.
[17] L.A. Fieber, D.J. Adams, J. Physiol. 434 (1991) 239–256.
[18] N. Mori, D. Wu, H. Furuta, Acta Otolaryngol. (Stockh.) 118 (1998) 192–197.
[19] O.P. Hamill, A. Marty, E.B. Neher, B. Sakmann, F.J. Sigworth, Pflügers Arch. 391 (1981) 85–100.
[20] K. Fukazawa, T. Matsunaga, H. Fujita, J. Clin. Electron. Microsc. 23 (1990) 135–147.
[21] G. Grynkiewicz, M. Poenie, R.Y. Tisen, J. Biol. Chem. 260 (1985) 3440–3450.
[22] C.A. Lewis, J. Physiol. 286 (1979) 417–445.
[23] Y. Yamashita, H. Ogawa, N. Akaike, Am. J. Physiol. 270 (1996) G307–G313.
[24] S.P. Soltoff, M.K. McMillian, B.R. Talamo, Am. J. Physiol. 262 (1992) C934–C940.
[25] J.G. Fitz, A.H. Sostman, Am. J. Physiol. 266 (1994) G544–G553.
[26] W. Walz, S. IIschner, C. Ohlemeyer, R. Banati, H. Kettenmann, J. Neurosci. 13 (1993) 4403–4411.
[27] S.C. Martin, J. Membr. Biol. 125 (1992) 243–253.
[28] D.J.B. Munoz, P.R. Thorne, G.D. Housley, T.E. Billett, Hear. Res. 90 (1995) 119–125.
[29] B.G. Mockett, X. Bo, G.D. Housley, P.R. Thorne, G. Burnstock, Hear. Res. 84 (1995) 177–193.
[30] D.J.B. Munoz, P.R. Thorne, G.D. Housley, T.E. Billett, J.M. Battersby, Hear. Res. 90 (1995) 106–118.
[31] D.C. Marcus, H. Sunose, J. Liu, Z. Shen, M.A. Scofield, Am. J. Physiol. 273 (1997) C2022–C2029.
[32] G.D. Housley, Mol. Neurobiol. 16 (1997) 21–48.